

# How does surface wettability influence nucleate boiling?

Hai Trieu Phan<sup>a,b,\*</sup>, Nadia Caney<sup>b</sup>, Philippe Marty<sup>b</sup>, Stéphane Colasson<sup>a</sup>,  
Jérôme Gavillet<sup>c</sup>

<sup>a</sup> LITEN/GRETh, CEA Grenoble, 17, rue des Martyrs, 38054 Grenoble cedex 9, France

<sup>b</sup> LEGI, BP 53, 38041 Grenoble cedex 9, France

<sup>c</sup> LITEN/LTS, CEA Grenoble, 17, rue des Martyrs, 38054 Grenoble cedex 9, France

Received 22 December 2008; accepted after revision 22 June 2009

Available online 24 July 2009

Presented by Jean-Baptiste Leblond

---

## Abstract

Although the boiling process has been a major subject of research for several decades, its physics still remain unclear and require further investigation. This study aims at highlighting the effects of surface wettability on pool boiling heat transfer. Nanocoating techniques were used to vary the water contact angle from 20° to 110° by modifying nanoscale surface topography and chemistry. The experimental results obtained disagree with the predictions of the classical models. A new approach of nucleation mechanism is established to clarify the nexus between the surface wettability and the nucleate boiling heat transfer. In this approach, we introduce the concept of macro- and micro-contact angles to explain the observed phenomenon. **To cite this article:** *H.T. Phan et al., C. R. Mecanique 337 (2009).*

© 2009 Académie des sciences. Published by Elsevier Masson SAS. All rights reserved.

## Résumé

**Effets de la mouillabilité sur l'ébullition en vase.** Cette étude a pour objectif d'étudier les effets de la mouillabilité sur l'ébullition en vase. L'angle de contact du fluide a été modifié par revêtement de nanoparticules sur des surfaces de test. Les résultats expérimentaux obtenus ne sont pas en accord avec les modèles classiques. Une nouvelle approche physique de l'influence de la mouillabilité sur l'ébullition en vase a été établie. Dans cette approche, nous introduisons les notions des macro- et micro-angles de contact afin d'expliquer les phénomènes observés. **Pour citer cet article :** *H.T. Phan et al., C. R. Mecanique 337 (2009).*

© 2009 Académie des sciences. Published by Elsevier Masson SAS. All rights reserved.

**Keywords:** Heat transfer; Wettability; Boiling; Contact angle; Nanocoating

**Mots-clés :** Transferts thermiques ; Mouillabilité ; Ébullition ; Angle de contact ; Revêtement nanostructuré

---

---

\* Corresponding author.

E-mail address: [hai-trieu.phan@cea.fr](mailto:hai-trieu.phan@cea.fr) (H.T. Phan).

### Nomenclature

$D_d$	bubble departure diameter, m	<i>Greek symbols</i>	
$f(\theta)$	energy factor	$\theta$	contact angle, °
$f_e$	bubble emission frequency, s <sup>-1</sup>	$\theta^\circ$	$\theta$ at 25 °C, °
$F_\sigma$	surface tension force, N	$\theta^s$	$\theta$ at saturated temperature, °
$F_{\sigma-h}$	horizontal component of $F_\sigma$ , N	$\theta_\mu^s$	micro-contact angle, °
$F_{\sigma-v}$	vertical component of $F_\sigma$ , N	$\rho$	density, kg/m <sup>3</sup>
$g$	gravity, m/s <sup>2</sup>	$\sigma$	surface tension, N/m
$h$	heat transfer coefficient, W/m <sup>2</sup> K	<i>Subscripts</i>	
$I$	current, A	$l$	liquid
$N_{as}$	number of active nucleation sites	$s$	saturation
$P$	pressure, bar	$v$	vapour
$q$	heat flux density, W/m <sup>2</sup>	$w$	wall
$S$	external area, m <sup>2</sup>	<i>Abbreviations</i>	
$T$	temperature, K	CHF	Critical heat flux
TCL	triple contact line	HTC	Heat transfer coefficient
$t_g$	growth time, s		
$t_w$	waiting time, s		
$V$	voltage, V		

## 1. Introduction

Nucleate boiling is characterized by the liquid–vapour phase change associated with the bubble formation. It is an effective heat transfer mode which occupies an important place in engineering disciplines. Compared to single-phase processes, this process enables to exchange more energy with a relatively lower temperature jump at the wall. During the last half of the twentieth century, significant advances were made in developing an understanding of the boiling heat transfer mode. Yet, because of the complexity of the process, the models and correlations developed often contain much simplification and could not explain recent observations. To explore the physics of the nucleate boiling process, further fundamental research is needed, especially on interfacial phenomena.

To date, the mechanism of heterogeneous nucleation still remains a major issue of two-phase heat transfer. Several investigations suggest that at the base of a bubble, the three phases: solid, liquid and vapour coexist in the so-called “triple contact line” (TCL). Does the surface wettability, which is defined through the contact angle of a liquid droplet on the wall, have significant influence on the bubble formation mechanism? Up to now, this issue has not been fully resolved for lack of experimental data. The effects of the surface wettability on nucleate boiling parameters are usually explained by several classical models such as Fritz [1], Wang and Dhir [2] and Kandlikar [3]. Balancing the buoyancy force and the vertical component of the surface tension force, Fritz [1] determined the bubble departure diameter. He obtained a linear variation of the bubble departure diameter with the contact angle. Wang and Dhir [2] have conducted boiling experiments with copper heaters oxidized at different degrees in order to vary the contact angle. The authors observed that increasing the surface wettability causes a decrease of the density of active nucleation sites. Analyzing the force resulting from the evaporation at the liquid–vapour interface of a bubble, Kandlikar [3] demonstrated that the increase of the surface wettability induced the enhancement of critical heat flux (CHF). Bao Truong et al. [4] combined these three models to show the mechanisms of the CHF intensification and heat transfer coefficient deterioration, both attributed to the decrease of the contact angle. In addition, as the TCL causes the discontinuities of the physical quantities, some studies avoid the TCL and suggest a continuous layer of non-evaporated liquid between the bubbles and the wall [5].

Up-to-now, few experimental data are available to clarify the controversial understandings about the effects of the surface wettability on boiling heat transfer. Indeed, it is experimentally difficult to vary the contact angle while keeping all other parameters constant. A typical way to change the contact angle is the use of surfactant solutions as described in Wen and Wang [6]. The disadvantage of this method is that both the surface wettability and the liquid surface tension

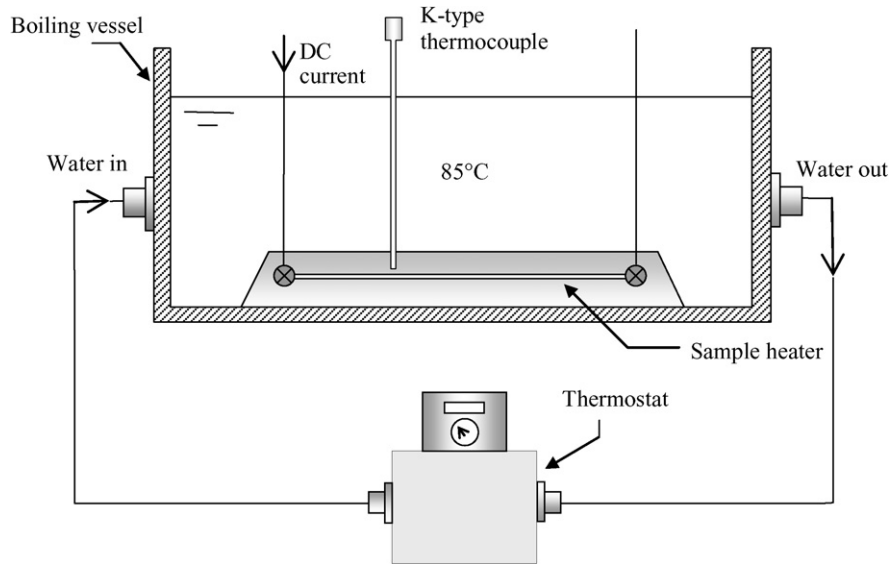
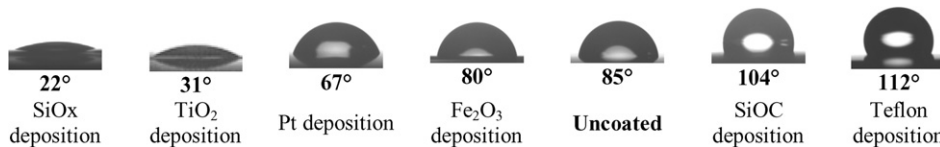


Fig. 1. Schematic view of the experimental setup.

Fig. 2. Static contact angles of a 2- $\mu$ L sessile water-droplet on stainless steel surfaces with and without nanoparticles deposition at 25 °C.

vary simultaneously. Hence, the enhancement of the boiling heat transfer might be due to the significant decrease of the liquid surface tension rather than the increase of the surface wettability. Another way is the surface treatment by microcoating such as the deposition of a microlayer of different materials on the heater surfaces [7–10]. However, this may disrupt the boiling process by changing the microcavities density on the heater. Oxidizing copper [11] is another method widely applied but this may also cause the change of the surface topography at microscale.

Today, the progress in nanocoating allows modifying surface topography and chemistry at nanoscale. Particles of very small size (less than 100 nm) named “nanoparticles” can be deposited on the heater surface. By changing the deposited particles material, it is possible to vary the water contact angle within 0° and 180°. As the characteristic scale of the nucleation sites is micrometric, only the contact angle is changed while all other boiling parameters would remain constant. The techniques used in this study are respectively MOCVD (Metal-Organic Chemical Vapour Deposition), PECVD (Plasma Enhanced Chemical Vapour Deposition) and NNBD (Nanofluids Nucleate Boiling Deposition). A pool boiling experiment was performed with the purpose of providing more experimental data to explore the influence of the surface wettability on the nucleate boiling mechanisms. A new physical approach of the nucleation is then established to understand the experimental results.

## 2. Experimental apparatus

The experimental setup is shown in Fig. 1. The initial surface is made of a 20  $\mu$ m stainless steel (grade 301) foil which has a water contact angle of about 85°. It was cut to make seven sample heaters 100 mm long, 5 mm wide. One of them has been used as reference of the uncoated surface. The others were coated either by MOCVD, PECVD or NNBD to obtain different water contact angle from 20° to 110° (Fig. 2). AFM (Atomic Force Microscope) scanning showed that in the initial state, the heater surfaces consist of parallel grooves 5  $\mu$ m wide and 100 nm deep. It is then expected that nanoparticles deposition with a thickness lower than 20 nm will not affect the surface microtopography. For each heater, the calibration of its electrical resistance as a function of the temperature was made beforehand. Hence, its temperature can be deduced from measurements of the electric resistance by using the elec-

Table 1  
Operating conditions and uncertainties.

Parameter	Operational range	Systematic uncertainty
$S$ (cm <sup>2</sup> )	10	3%
$V$ (V)	5–20	0.008–0.011%
$I$ (A)	5–20	0.010–0.015%
$P$ (bar)	1	±0.01
$T_s$ (°C)	100	±0.2
$T_w$ (°C)	100–150	±1
$q$ (kW/m <sup>2</sup> )	50–400	3%
$h$ (W/m <sup>2</sup> K)	3000–16 000	10–20%

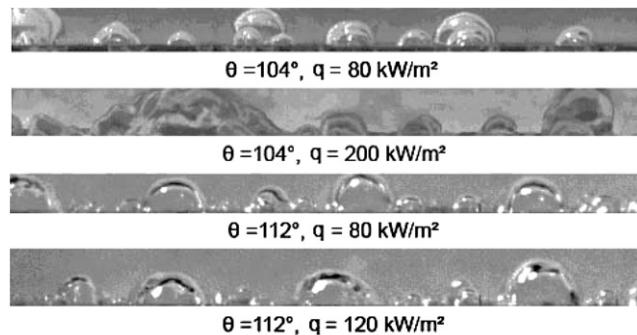


Fig. 3. For the hydrophobic surfaces, the bubbles appeared at very low superheats, but they could not detach from the wall. There was no nucleation and a film boiling configuration rapidly occurred because of the bubble coalescence.

trical resistance/temperature curve. The sample heater was put in a boiling vessel containing pure water at 85°C. It was placed in horizontal orientation. The water temperature inside the vessel was maintained constant by a flow at very low flow rate from a thermostat. The sample heater was then heated by Joule effect to boil water near the heater surface. Boiling occurs on both sides of the sample heater. The experiment was done at atmospheric pressure. During the experiment, the boiling process was captured by a high speed camera with a recording speed of 6000 fps. Table 1 shows the measurement uncertainties estimated by error propagation approach.

### 3. Experimental results

#### 3.1. Hydrophobic surfaces

Fig. 3 presents some captured images of the boiling process on the hydrophobic surfaces whose static contact angles at 25 °C are respectively 104 and 112° (Fig. 2). Compared to the standard surfaces which are usually wetted, the bubbles appeared on the hydrophobic surfaces at a lower heat flux. Increasing the heat flux, the bubble size increased but the bubbles still did not detach from the wall. In fact, no bubble emission was observed on the hydrophobic surfaces. At higher heat flux, the bubbles spread over the surfaces, causing bubble coalescence that led to film boiling. These observations agree with those of Gaertner [8] and Hummel [9]: a continuous hydrophobic surface tends to become vapour blanketed during nucleate boiling. However, no bubble departure was noticed and the heat transfer was not stable when the bubbles stayed on the heater surfaces. The wall temperature increased with time and after about fifteen minutes, local wall destruction occurred. Thus, it was impossible to measure the HTC in stationary regime.

#### 3.2. Hydrophilic surfaces

By analyzing the photos taken from the videos recorded by the high speed camera, we determined the bubble departure diameter ( $D_d$ ) and the bubble emission frequency ( $f_e$ ) for each hydrophilic surface. Fig. 4 shows that a

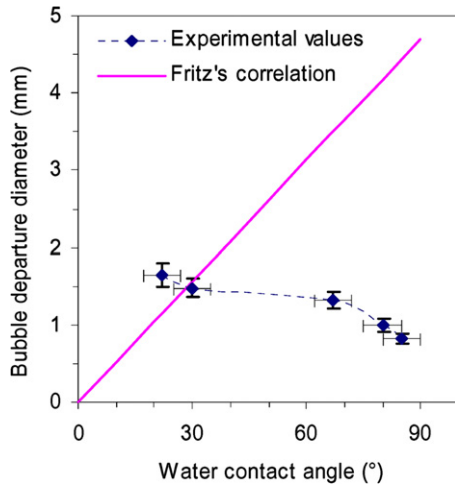


Fig. 4. Bubble departure diameter versus the contact angle measured at 25 °C.

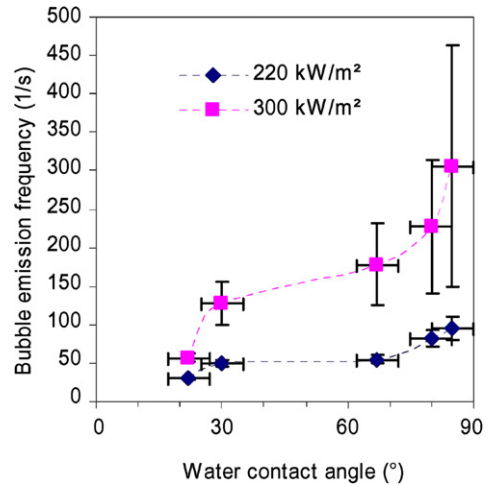


Fig. 5. Bubble emission frequency versus the contact angle measured at 25 °C.

greater surface wettability yields bigger bubble departure diameter. This is in contrast with the correlation of Fritz [1] which estimates that  $D_b$  is proportional to the static contact angle. Furthermore, the duration of the bubble growth ( $t_g$ ) and the time interval between the departure of each bubble and the appearance of the next bubble ( $t_w$ ) were determined. It is logical to imagine that the formation of a bigger bubble requires a longer time. This is what we observed. Indeed, the decrease of the contact angle resulted in the increases of both  $t_g$  and  $t_w$ . As a consequence, the bubble emission frequency, which is defined as  $f_e = 1/(t_g + t_w)$ , decreases with the enhancement of the surface wettability (Fig. 5).

The measurement of the density of active nucleation sites ( $N_{as}$ ) has been known to be difficult. To obtain reliable values, the heater surfaces must be uniform in terms of the number and the size of the nucleation sites. On a large surface, this condition would never be satisfied. But the information about  $N_{as}$  is useful to interpret the effects of the surface wettability on heat transfer. The high speed camera was positioned so that it provides a perspective view of the bubble generation. Then,  $N_{as}$  was determined on a heater part 23 mm wide. We observed that at a given moment,  $N_{as}$  decreased with the enhancement of the surface wetting. This is in agreement with what was described by Wang and Dhir [2]. However, when  $N_{as}$  was averaged over a long period (1 s), it remained almost independent of the contact angle (Fig. 6). Fig. 7 represents the variation of the heat transfer coefficient as a function of contact angle. It shows that  $h$  deteriorates with the decrease of the contact angle when the latter is within 30 and 90°. Yet, when the contact angle is lower than 30°, its decrease induces an increase of  $h$ . While working on superhydrophilic surfaces, Takata et al. [12] have observed the same phenomenon. These authors used dipping and sputtering techniques to deposit titanium dioxide ( $\text{TiO}_2$ ) on smooth surfaces. Then, the coated surfaces were oxidized by ultraviolet radiation, creating the  $\text{TiO}_2$  photocatalysis that enables to obtain a water contact angle near 0°. Some points extracted from their experimental results are shown in Fig. 7. They follow the trend of the curves fitting our results relatively well. Hence, the best heat transfer coefficient would be obtained with a surface of which the contact angle of is either 0 or 90°.

#### 4. Physical approach

Our experimental results showed a significant influence of the surface wettability on the nucleated boiling. In particular, a clear difference of the bubble formation mechanism was observed between the hydrophobic and hydrophilic surfaces. The contact angle is usually measured at room temperature (25 °C) by depositing a liquid droplet on the sample surface. The surface and the droplet are at the same temperature, thus there is no heat exchange between them. This contact angle is denoted as  $\theta^\circ$ . However, during the nucleate boiling, the bubble is formed by the liquid evaporation caused by the heat transfer from the wall to the liquid. The contact angle that follows ( $\theta_s$ ) is different from  $\theta^\circ$ , because the liquid is now at saturated temperature (Fig. 8). In general, the liquid surface tension decreases with the increase of the temperature. Hence,  $\theta_s$  is lower than  $\theta^\circ$  when the saturated temperature is higher than that of

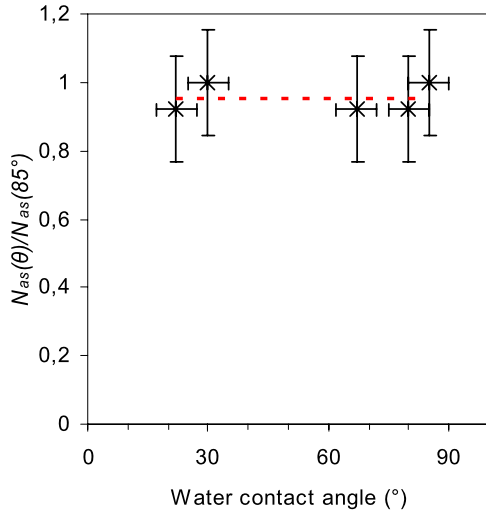


Fig. 6. Ratio of  $N_{as}$  (averaged during 1 s on a heater part 23 mm wide) versus the contact angle measured at 25 °C.

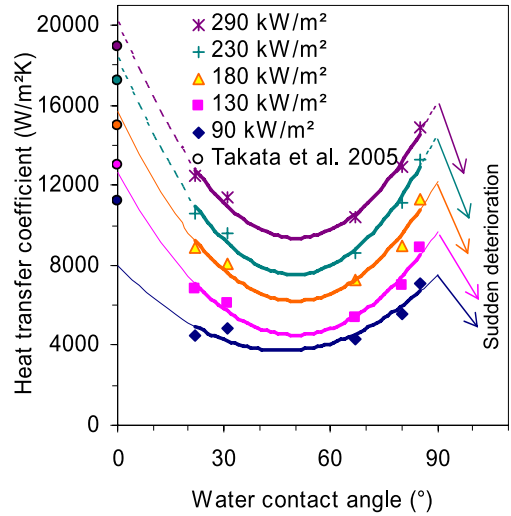


Fig. 7. Heat transfer coefficient versus the contact angle measured at 25 °C.

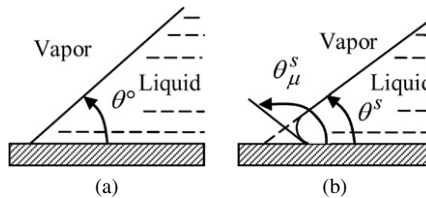


Fig. 8. (a) Contact angle of a liquid droplet at 25 ° without any heat transfer; (b) Contact angles of the bubble formed when the wall is heated: macro-contact angle  $\theta^s$  and micro-contact angle  $\theta_{\mu}^s$ .

the room. In addition, at boiling conditions, the balance of the three surface energies: solid–liquid, liquid–vapour and solid–vapour, becomes unstable due to the non-zero heat flux imposed at the solid–liquid interface. For the hydrophilic surfaces, this heat flux causes the evaporation of the liquid micro-layer underneath the bubble. The thinner this layer is, the higher the heat flux passing through. Close to the TCL, the heat transfer would be extremely high and would create a liquid evaporation with a rate that is much higher than in the surrounding areas. Therefore, the curvature of the liquid–vapour interface would change, leading to the emergence of another contact angle named “micro-contact angle” ( $\theta_{\mu}^s$ ). The contact angle  $\theta_s$  is relatively at a larger scale. It is named “macro-contact angle”.

4.1. Influence of the micro-contact angle

The surface tension force ( $F_{\sigma}$ ) is determined by the micro-contact angle and not by the macro-contact angle. When the nucleation is initiated, close to the TCL, the liquid evaporation may cause a micro-contact angle greater than 90°, as described by Mitrovic [13]. Due to the horizontal component of the surface tension force ( $F_{\sigma\_h}$ ), the liquid in the micro-layer moves backward from the bubble axis and the TCL expands from A to B (Fig. 9). Along with the liquid movement, the micro-contact angle decreases as a result of the restoration of the surface energies balance. At position B, the micro-contact angle is equal to 90° and the surface tension force stops displacing the TCL. However, the liquid inertia and the energy minimization of the system will result in a decline of the micro-contact angle to a value close to that of the macro-contact angle. The horizontal component of the surface tension force reappears, but this time it moves the liquid forward by reducing the TCL radius. At position C, the TCL disappears and the bubble detaches from the wall.

The micro-contact angle is an important parameter in nucleated boiling. First, it directly affects the vertical component of the surface tension force ( $F_{\sigma\_h}$ ), which contributes to maintain the bubble on the wall. Then, it creates the TCL movement and thus affects the dynamic forces caused by the liquid inertia and viscosity. Indeed, when the

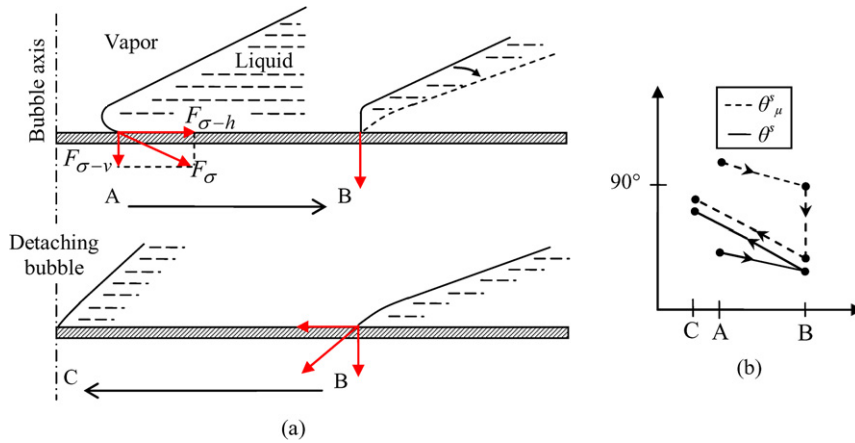


Fig. 9. (a) Nucleation initiation creates a micro-contact angle greater than  $90^\circ$ , causing the displacement of the TCL from A to B. At position B, the horizontal component of the surface tension force becomes zero, but the liquid inertia and the energy minimization of the system induces the decrease of the micro-contact angle to a value close to that of the macro-contact angle. Due to the surface tension force, the TCL retracts. Its radius tends to zero at C, enabling the bubble departure. (b) The change of the macro- and micro-contact angles during bubble growth.

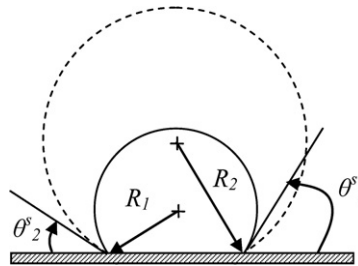


Fig. 10. Two spherical bubbles are assumed to have the same TCL. If  $\theta_2^s$  is lower than  $\theta_1^s$ , the bubble whose contact angle is  $\theta_2^s$  is bigger than that having the contact angle  $\theta_1^s$ .

TCL is expanding from A to B, the bubble becomes bigger and the inertia of the liquid surrounding the bubble exerts a reaction force to maintain it on the wall. But when the TCL retracts from B to C, the liquid goes forward to the bubble axis, enabling the bubble departure. During the bubble growth, the macro-contact angle changes according to the hysteresis phenomenon: it decreases when the liquid recedes and increases when the liquid advances.

#### 4.2. Influence of the macro-contact angle

Although the surface tension force depends on the micro-contact angle, the macro-contact angle always plays a key role. A simple way of understanding the effects of the macro-contact angle is to analyze its influence on the bubble form. The initial radius of the TCL is assumed to be equal to that of the nucleation sites. At the same TCL, for a simple geometry reason, the bubble which has a lower contact angle is bigger (Fig. 10). This might explain why the increase of the surface wettability leads to the increase of the energy required to activate the nucleation sites. Therefore, between the departure of a bubble and the appearance of the next one, the waiting time ( $t_w$ ) would be longer when the macro-contact angle is lower. The decrease of the macro-contact angle would then intensify the phase difference caused by the time delay between the active nucleation sites (two nucleation sites are said to be “in phase” if they emit the bubbles at the same time). That might explain why, at a given time, while increasing the contact angle, we observed fewer active nucleation sites, whereas if the observation is made over a long period,  $N_{as}$  remained almost independent of the macro-contact angle. Moreover, when the bubble is bigger, its growth time ( $t_g$ ) increases. Hence, the increases of both  $t_w$  and  $t_g$  induce the decrease of the bubble emission frequency. Bankoff [14] defined the energy factor,  $f(\theta)$ , as the ratio of the energy needed to form a bubble with a contact angle  $\theta$  to that needed to form a homogeneous bubble with the same diameter. Its expression is given by:

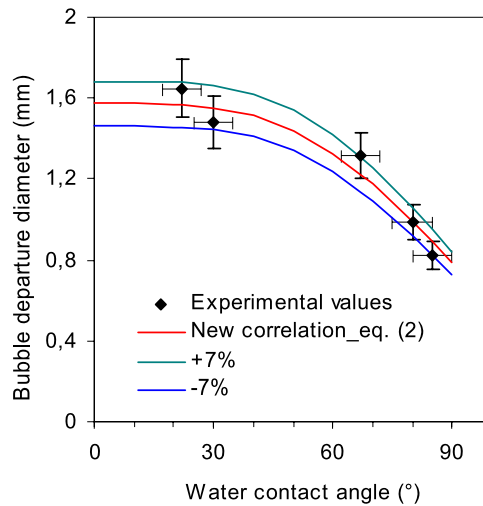


Fig. 11. New correlation to estimate the bubble departure diameter.

$$f(\theta) = \frac{2 + 3 \cos \theta - \cos^3 \theta}{4} \quad (1)$$

This factor is simply the volume ratio between a truncated sphere of which the contact angle is  $\theta$  and a full sphere which has the same diameter. It could be representative for the influence of the macro-contact angle on the bubble form. Thereby, we established a new correlation of the bubble departure diameter which incorporates the influence of the fluid properties and gravity as Fritz [1] did, but takes into account the energy factor as the contribution of the wetting effects:

$$D_d = 0.626977 \times \frac{(2 + 3 \cos \theta - \cos^3 \theta)}{4} \left( \frac{\sigma}{g(\rho_l - \rho_v)} \right)^{1/2} \quad (2)$$

Fig. 11 shows that this new correlation fits the experimental results relatively well with only 7% difference.

Furthermore, the macro-contact angle affects the heat transfer through its effect on the liquid micro-layer underneath the bubble. For a lower macro-contact angle, this area would be thinner and larger, improving  $h$ . Thus, the results shown in Fig. 7 could be explained by analyzing the compromise between the effect on  $f_e$  and that on the liquid micro-layer. At  $90^\circ$  macro-contact angle, there is an optimum of  $h$  as  $f_e$  is maximum. When the macro-contact angle is within  $30^\circ$  and  $90^\circ$ , the effect on  $f_e$  dominates and the decrease of  $f_e$  (due to the decrease of the macro-contact angle) causes the deterioration of  $h$ . However, when the macro-contact angle is lower than  $30^\circ$ , the effect on the liquid micro-layer dominates. Despite the fact that  $f_e$  is the lowest, at  $0^\circ$  macro-contact angle, the bubbles stay longer on the heater surface with the largest and thinnest liquid micro-layer, inducing another optimum of  $h$ .

Through its influence on the liquid micro-layer, the macro-contact angle also affects the micro-contact angle and especially the movements of the TCL. For a lower macro-contact angle, the expansion of the TCL would be longer but its retraction would be faster. We believe that the speed of the liquid advancing when the TCL goes from B to C (Fig. 9) would play an important role in the CHF enhancement mechanism. In fact, the CHF might be improved if this speed becomes higher, for example by increasing the capillary length of the coating. This might explain why at the same contact angle, Kim et al. [15] observed a better CHF for more porous coating.

Fig. 12 summarizes the effects of the macro-contact angle on the nucleated boiling.

## 5. Conclusion

Our experimental results showed that the surface wettability has significant effects on the nucleated boiling. They tend to prove the existence of the triple contact line at the base of the bubbles. Near this line, because of the ultra-high rate of liquid evaporation, the curvature of the liquid–vapour interface changes, causing a change of the contact angle. Thus, we distinguish micro- and macro-contact angles. Due to the micro-contact angle, the TCL expands and

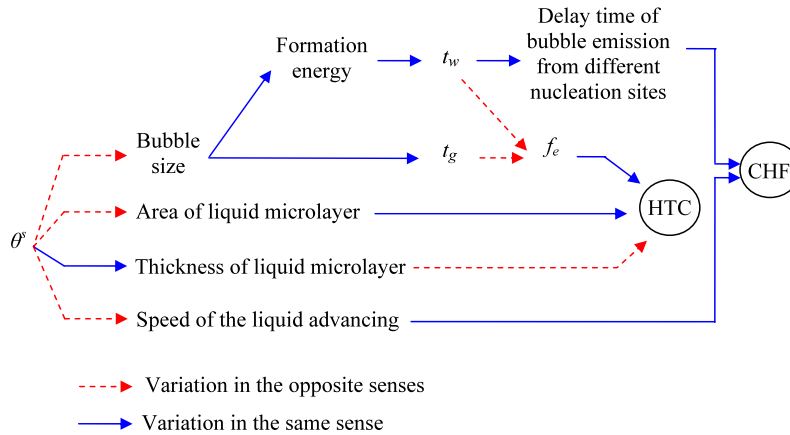


Fig. 12. Logical diagram describing the effects of the macro-contact angle on the nucleated boiling parameters.

then retracts during the bubble growth, creating the liquid movements that are responsible for the macro-contact angle hysteresis and the bubble departure. The influence of the macro-angle on the bubble form has been analyzed to explain the experimental observations, especially those concerning the heat transfer coefficient and the critical heat flux.

## References

- [1] W. Fritz, Maximum volume of vapour bubbles, *Phys. Z.* 36 (1935) 379–384.
- [2] C.H. Wang, V.K. Dhir, Effect of surface wettability on active nucleate site density during pool boiling of water on a vertical surface, *Trans. ASME J. Heat Transfer* 115 (1993) 670–679.
- [3] S.G. Kandlikar, A theoretical model to predict pool boiling FC incorporating effects of contact angle and orientation, *J. Heat Transfer* 123 (2001) 1071–1079.
- [4] B. Truong, L.W. Hu, J. Buongiorno, Surface modifications using nanofluids for nucleate boiling heat transfer, ICNMM2008-62085, Darmstadt, Germany, 2008.
- [5] Y.A. Buyevich, B.W. Webbon, Dynamics of vapour bubbles in nucleate boiling, *Int. J. Heat Mass Transfer* 39 (1996) 2409–2426.
- [6] D.S. Wen, B.X. Wang, Effects of surface wettability on nucleate pool boiling heat transfer for surfactant solutions, *Int. J. Heat Mass Transfer* 45 (2002) 1739–1747.
- [7] P. Griffith, J.D. Wallis, The role of surface conditions in nucleate boiling, *Chem. Eng. Prog. Symp. Ser.* 56 (1960) 49–63.
- [8] R.F. Gaertner, Methods and means for increasing the heat transfer coefficient between a wall and boiling liquid, U.S. Patent 3,301,314 (1967).
- [9] R.L. Hummel, Means for increasing the heat transfer coefficient between a wall and boiling liquid, U.S. Patent 3,207,209 (1965).
- [10] R.I. Vachon, G.H. Nix, G.E. Tanger, Evaluation of constants for the Rohsenow pool-boiling correlation, *J. Heat Transfer* 90 (1968) 239–247.
- [11] S.C. Johnathan, J. Kim, Nanofluid boiling: The effect of surface wettability, *Int. J. Heat Mass Transfer* 29 (2008) 1577–1585.
- [12] Y. Takata, S. Hidaka, J.M. Cao, T. Nakamura, H. Yamamoto, M. Masuda, T. Ito, Effect of surface wettability on boiling and evaporation, *Energy* 30 (2005) 209–220.
- [13] J. Mitrovic, Formation of a liquid jet after detachment of a vapour bubble, *Int. J. Heat Mass Transfer* 40 (1997) 4309–4317.
- [14] S.G. Bankoff, Ebullition from solid surfaces in the absence of a pre-existing gaseous phase, *Trans. Am. Mech. Eng.* 79 (1957) 735–740.
- [15] H. Kim, M. Kim, Effect of nanoparticle deposition on capillary wicking that influences the critical heat flux in nanofluids, *Appl. Phys. Lett.* 91 (2007) 014104.